ACS APPLIED MATERIALS & INTERFACES

Research Article

www.acsami.org

Uniform Ultrasmall Graphene Oxide Nanosheets with Low Cytotoxicity and High Cellular Uptake

Huan Zhang,[†,‡] Cheng Peng,[†,‡] Jianzhong Yang,[†] Min Lv,[†] Rui Liu,[*,§] Dannong He,[§] Chunhai Fan,[†] and Qing Huang[*,†]

[†]Laboratory of Physical Biology, Shanghai Institute of Applied Physics, Chinese Academy of Sciences, Shanghai 201800, China

[§]National Engineering research Center for Nanotechnology (NERCN), Shanghai 200241, China

Supporting Information

ABSTRACT: Graphene oxide (GO) is an increasingly important nanomaterial, which exhibits great promise in the area of bionanotechnology and nanobiomedicine. In this study, we synthesized uniform ultrasmall graphene oxide nanosheets with high yield by a convenient way of modified Hummers' method. The uniform ultrasmall GO nanosheets, which exhibit fluorescence property and outstanding stability in a wide range of pH values, were less than 50 nm. Furthermore, because of the advantages of its lateral size, the uniform ultrasmall GO nanosheets showed excellent biocompatibility of lower cytotoxicity and higher cellular uptake amount compared to the random large GO nanosheets. Therefore, the as-prepared uniform ultrasmall GO nanosheets could be explored as the ideal nanocarriers for drug delivery and intracellular fluorescent nanoprobe.

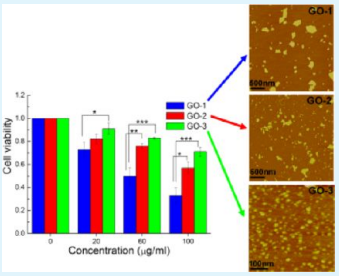

KEYWORDS: *graphene oxide, ultrasmall, stability, cytotoxicity, cellular uptake, nanocarrier*

INTRODUCTION

Graphene, as a one-atom-thick two-dimensional carbon nanosheet,[1−4] has attracted great attention and shown great potential applications for electronics,[5,6] nanocomposites,[7−10] sensors,[11−15] nanocarriers,[16,17] and energy sources[18,19] for its amazing physical properties.[20,21] Graphene oxide (GO),[22,23] the oxidized form of graphene, has been widely studied in the field of cell biology[24−28] for its outstanding biocompatibility, large surface, and convenient chemical modification.[29−32] Besides, several groups have reported that GO nanosheets could serve as nanocarriers to deliver drugs,[33,34] nucleic acids,[35] or other biomolecules[16] into cells or mice[36] for bioimaging,[37,38] biosensing,[13,39,40] and therapeutic purposes.[41,42] For instance, fluorescence modified GO can be applied as pH-tunable fluorescent nanoprobe for intracellular imaging;[28] PEI-grafted GO can be used to deliver SiRNA and drugs;[24] polyethylene glycol grafted GO can be applied as a useful nanovehicle of drug delivery for cancer therapy.[34]

In common sense, uniform sized nanomaterials with diameters less than 100 nm are more suitable for intracellular applications such as imaging and drug delivery. However, GO nanosheets are often economically prepared by Hummers' method, and the lateral size of the as-prepared GO by this random "top-down" chemical exfoliation from graphite powder is quite polydispersed, ranging from tens of nanometers to even a few micrometers. Therefore, efforts towards obtaining uniform sized GO nanosheets with diameters less than 100 nm have recently been reported by density gradient ultracentrifugal rate separation[43] and pH-assisted selective sedimentation.[44] However, their methods were based on the separation technology and inevitably led to low yield. Huang et al.[45] synthesized uniform GO nanosheets with lateral size smaller than 100 nm by chemical exfoliation of crystalline graphite nanofibers, but one point must be noticed is that crystalline graphite nanofiber is not economical enough as a starting material and would increase the cost of GO nanosheets. Moreover, Liu et al.[34] reported a kind of PEGylated Nano GO for delivery of water-insoluble cancer drugs. However, according to our previous work,[46] PEGylation would significantly reduce the adsorption ability of GO nanosheets, and that would not do any good for GO as a nanocarrier. Uniform GO nanosheets were quite important and were eagerly needed for biological applications; however, there is not an appropriate method to synthesize them until now.

Recently, Tour et al.[47] studied the chemical mechanism of GO nanoribbons' preparation and pointed out that the $KMnO_4$−H_2SO_4 treatment was just like the "scissors" that could cut stacks of graphite into smaller GO nanosheets. Inspired by their work, we presumed that after several rounds of $KMnO_4$−H_2SO_4 oxidation, the lateral size of GO nanosheets would turn out to be smaller and the size distribution would be more uniform. Herein, based on Hummers' method,[48] we developed a high yield, low-cost, convenient method via several rounds of oxidation for preparing uniform GO nanosheets with lateral size less than 50 nm, using normal graphite powder as starting material. This uniform sized ultrasmall GO nanosheets have excellent fluorescent property and stability in different pH buffer solutions. More interestingly, they exhibit better

Received: December 6, 2012
Accepted: February 13, 2013
Published: February 13, 2013

   dx.doi.org/10.1021/am303005j | ACS Appl. Mater. Interfaces 2013, 5, 1761−1767

biocompatibility and higher cellular uptake efficiency compared to the random distributed lateral sized GO nanosheets. These excellent properties endow them with great potential applications as ideal nanocarriers of anticancer drugs or active biological molecules in many frontier fields, such as cell biology and molecular medicine.

RESULTS AND DISCUSSION

Preparation and Characterization of Uniform Ultrasmall GO Nanosheets. Modified Hummers' method was used to synthesize GO-1 nanosheets, and repeated oxidation was facilitated to cut GO-1 into smaller GO-2 and GO-3 nanosheets with a high yield of 90%, 80%, and 65% of GO-1, GO-2, and GO-3, respectively. The morphologies of GO-1, GO-2, and GO-3 nanosheets were investigated by transmission electron microscopy (TEM) and atom force microscopy (AFM). TEM images of GO-1, GO-2, and GO-3 were shown in Figure 1a, b, and c. Even though the shapes of GO-1 and GO-2 sheets were similar as previous reports, the shape of GO-3 was quite different in two facets. One was that the lateral size of GO-3 nanosheets was uniform and less than 50 nm; the other was that after three times of heavy oxidization, the edges of GO-3 nanosheets were quite wrinkled, but the middle areas were well maintained in status of GO nanosheets. Atomic force microscopy (AFM) images of three types of GO nanosheets were further shown in Figure 1d, e, and f. The lateral sizes of GO-1, GO-2, and GO-3 were quite different though their thicknesses were all about 1.1 nm. As shown in Figure 1d, the lateral size of GO-1 was randomly ranging from hundreds of nanometer to several micrometers. In Figure 1e, the lateral size of GO-2 nanosheets was in the range of hundreds of nanometers, but many small sized GO nanosheets appeared, owning to two times of oxidization. Dramatically, after three times of oxidization, the lateral size of GO-3 nanosheets was quite narrow, less than 50 nm (Figure 1f.) The dynamic light scattering (DLS) method was employed to determine the quantitative hydrodynamic diameters of GO nanosheets in aqueous solution after centrifugation at 10000 rpm for 10 minutes of each samples; the average lateral size of GO-1, GO-2, and GO-3 was 205.8 nm, 146.8 nm, and 33.78 nm, respectively (Figure S2). According to the work of Wang et al.,[50] GO colloids were stable only when zeta potential was below −30 mV. Therefore, the stability of different lateral sized GO colloids at different pH values was studied by zeta potential measurement. As shown in Table S1, GO-3 colloids showed the most negative potential and thus exhibited the best stability. Furthermore, zeta potentials of all GO colloids increased as the pH value decreased,[45] and the GO-1 colloid even aggregated and deposited from the solution when the pH value was adjusted to lower than 6. However, GO-3 colloids' zeta potential kept below −30 mV when the pH values were in a wide range from 10 to 4, which indicated that GO-3 colloid was more stable than GO-1 or GO-2 colloids.

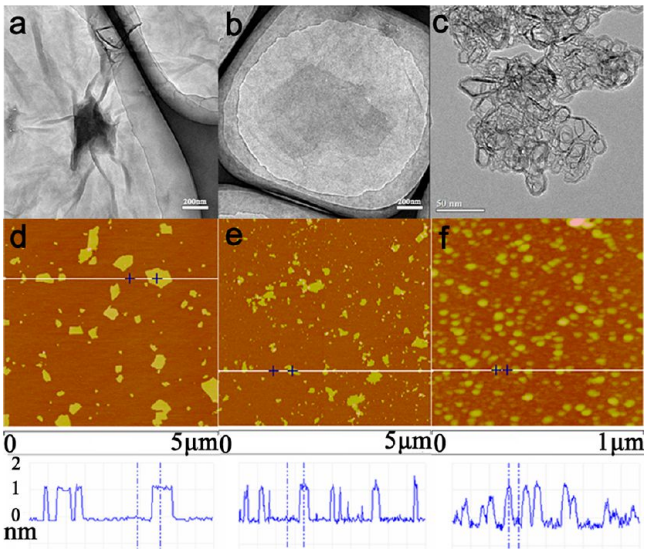

Figure 1. Characterizations of GO nanosheets. TEM images of GO-1(a), GO-2 (b), GO-3 (c) and AFM images of GO-1(d), GO-2 (e), GO-3 (f).

More characters of GO-1, GO-2, and GO-3 nanosheets were studied by X-ray photoelectron spectroscopy (XPS), Fourier Transform Infrared spectroscopy (FTIR), and Raman spectroscopy. In detail, the peaks at 1620 cm^{-1}, 1062 cm^{-1}, and 1720 cm^{-1} were corresponding to the stretching vibrations of C═C, C−O−C, and C═O groups, respectively,[49] which indicated the sp^2 domains of carbon atoms were reserved even though many oxygenated groups were introduced on the graphene sheets after three times of oxidization (Figure S3). However, the XPS spectra revealed that the relative contents of different oxygenated groups were obviously changed after different oxidation times. As shown in Figure 2a, b, and c, the ratio of C−O vs O═C−O was decreased from more than 2:1 to less than 1:1 when the oxidation times increased, which indicated the oxidation degree was higher and more carboxyl groups were generated at the edge of graphene nanosheets. These carboxyl groups would be ionized H^+ in aqueous solution, while the COO^- groups were left on the surface of GO nanosheets, which would certainly make the zeta potential of GO nanosheets more negative. Because of the effects of charge exclusion, the nanomaterials with more negative zeta potential always exhibited better stability in aqueous solution. Therefore, the result of increasing O═C−O groups on GO nanosheets after repeated oxidization could also be used to well explain the lower zeta potential and the better stability of GO-3 colloid in a wide range of pH values. Furthermore, the hypsochromic shift (from 1360.9 cm^{-1} of GO-1 to 1369.5 cm^{-1}) of the D bond in Raman spectra (Figure S4) of GO-3 as well as the value of ID/IG was decreased from 1.06 of GO-1 to 0.96 of GO-3, all of which indicated more defects were introduced into the graphene nanosheets after three times of oxidization.[50] Moreover, GO-3 nanosheets emitted strong fluorescence at 520 nm when excited at 400 nm (Figure 2d), which is almost six times stronger than GO-1 nanosheets in the same concentration. According to tunable photoluminescence property of graphene oxide by Chien et al.[51] integrating with their small size, GO-3 nanosheets might be employed as promising intracellular fluorescent nanoprobe or intracellular biosensors, etc.

Cellular Uptake and Cytotoxicity. As we all know, carbon nanomaterials such as fullerene,[52,53] nanodiamond,[54] and carbon nanotubes[55] have great biological applications and can serve as nanocarriers to effectively deliver drugs, nucleic acids, proteins, and other molecules into cells. Graphene, as a newly discovered carbon nanomaterial, has drawn great attentions due to its unique properties. Graphene oxide (GO), an oxygenated graphene derivative, with better biocompatibility, has been profoundly explored for biomedical applications such as in vitro

dx.doi.org/10.1021/am303005j | ACS Appl. Mater. Interfaces 2013, 5, 1761−1767

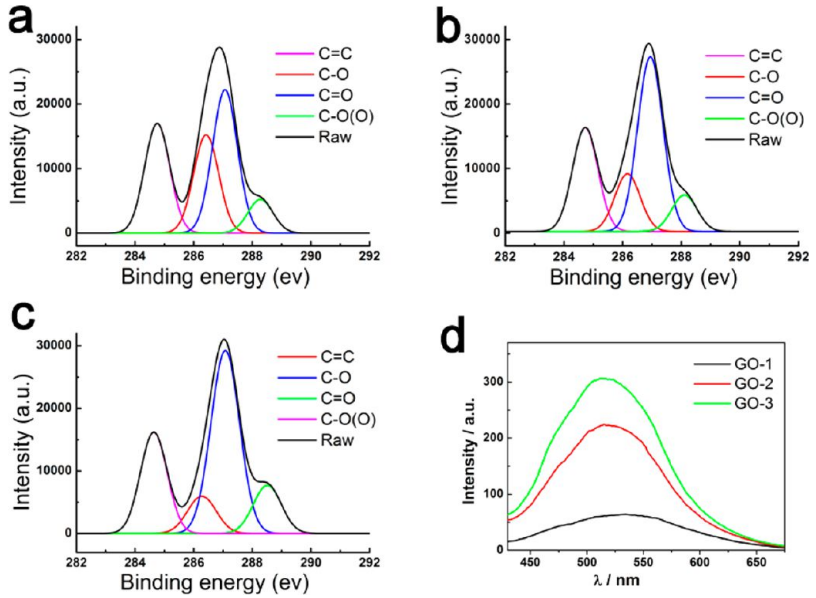

Figure 2. XPS spectra of GO-1(a), GO-2 (b), GO-3 (c) and fluorescence spectra of the three GO sheets (EX = 400 nm).

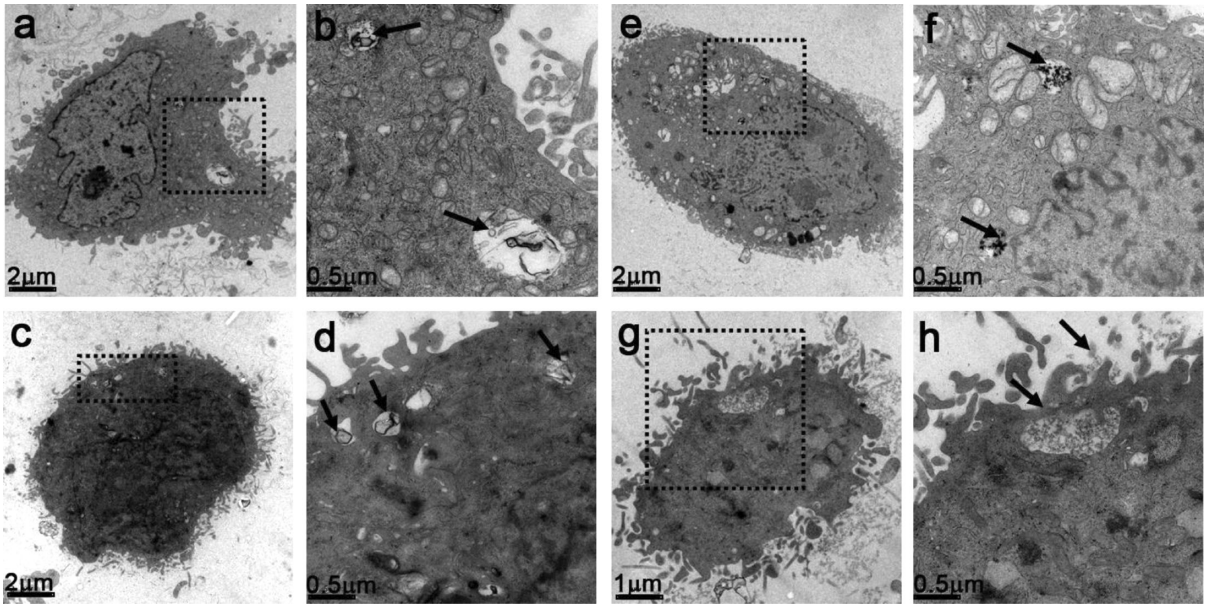

Figure 3. TEM images of Hela cells showing the internalization of GO nanosheets. (a, b), (e, f) are images of Hela cells incubated 2 h with 100 μg/mL GO-1 or GO-3, and (c, d), (g, h) are images of Hela cells incubated 24 h with 20 μg/mL GO-1 or GO-3. (b, d, f, and h are the relative magnified regions of a, e, c, and g; the black arrows point to the materials).

drug delivery and cellular imaging. However, one thing must be assured is that GO nanosheets could be internalized by cells. Since different lateral sized GO nanosheets have been synthesized, their behaviours in cell biology would be more interesting. Mu et al. pointed that GO nanostructures with protein coating were able to adhere on cell surface and undergo size-dependent internalization.[56] According to our results, both GO-1 and GO-3 nanosheets could be enwrapped by elongated Hela cells synapses and be internalized within Hela cells via endocytosis. TEM images of Hela cells (Figure 3) clearly demonstrated the cellular uptake of both GO-1 and GO-3 nanosheets could happen in different concentration (20 or 100 μg/mL) and different incubation time (2 or 24 h), and this was also supported by the aggregates of GO-1 and GO-3 nanosheets in cytoplasm.

According to TEM results, GO nanosheets could easily be uptaken by Hela cells. However, quantitative determination of the amount of cellular uptake of different GO nanosheets was desirable. Therefore, labeling and tracing techniques with a radionuclide were used in the study. GO-1, GO-2, GO-3 nanosheets, Single-Walled Carbon Nanotubes (SWCNTs), and Multi-Walled Carbon Nanotubes (MWCNTs) were labeled by radioactive ^{125}I to determine the amount of intracellular uptake by isotope labeling method. The final concentration of all ^{125}I-labeled materials was 20 μg/mL, and the incubation time was 2 h or 24 h, respectively. The relative uptake percentage of ^{125}I-labeled GO nanosheets and the detailed amount were shown in Figure 5. The uptake percentages of 8.94% and 6.08% of GO-3 and GO-2 after 2 h were significantly higher than GO-1. Besides, the uptake percentage of 14.97% after 24 h of GO-3

dx.doi.org/10.1021/am303005j | ACS Appl. Mater. Interfaces 2013, 5, 1761−1767

nanosheets was significantly higher than GO-1 and GO-2, respectively; all of these directly indicated that the uptake quantity was closely related to the lateral size of GO nanosheets. Consequently, we calculated the uptake quantities of the materials per 10000 cells (ng/10000 cells, see details in Table 1), and the results were consistent with our speculation

Table 1. Cellular Uptake Quantities of ^{125}I Labeled Five Different Materials[a]

	incubation time			
	2 h		24 h	
materials	percentage	ng/10000 cell	percentage	ng/10000 cell
GO1	3.63%	36.3	8.20%	328.0
GO2	6.08%	60.8	10.72%	428.8
GO3	8.94%	89.4	14.97%	598.8
SWNT	1.47%	14.7	8.49%	339.6
MWNT	4.91%	49.1	7.07%	282.8

[a]All data shown are the means of three samples.

about size-dependent uptake too. As a result, the smaller the lateral size of GO nanosheets was, the easier the uptake by Hela cells was. In addition, the uptake percentages of all different lateral sized GO nanosheets were higher than SWCNTs and MWCNTs, which indicated that the GO nanosheets were much easier to uptake by mammalian cells and might be more suitable for antidrug nanocarriers.

Next, to further study the impact of different GO nanosheets on cells and whether the cell cytotoxicity was related to the lateral size of GO nanosheets, classic MTT viability assays were employed to evaluate and compare the cytotoxicity of the GO nanosheets on Hela cells. Based on our previous work,[57] proteins in cell medium would absorb to GO nanosheets and would mitigate the cell cytotoxicity by lessening the contact between GO nanosheets and cells,[46] so the FBS proportion in culture medium was reduced from 10% to 1% in order to eliminate the influence of proteins and directly evaluate the cellular uptake behaviour and cytotoxicity caused by GO nanosheets.

As shown in Figure 4, compared to GO-1, GO-2 and GO-3 nanosheets exhibited significantly lower cytotoxicity towards Hela cells than GO-1 after incubation for 2 h or 24 h, directly indicating that the cytotoxicity was size-dependent of GO nanosheets. However, when the incubation time was up to 24 h, the differences were not obvious. According to the previous research of interactions between bacteria and graphene or graphene oxide,[58,59] the cytotoxicity might be caused by the physical damage derived from GO nanosheets. Given the relative lateral size of the three GO nanosheets, we proposed that small sized GO nanosheets might damage the cell membrane more slightly than large sized GO nanosheets. However, we believed that the cytotoxicity was more than a result of physical damage to the cell membrane. According to Table 1, when incubation time was up to 24 h, GO-2 and GO-3 have a much higher uptake amount than GO-1, thus uptake of the GO nanosheets could cause changes in the microenvironment of cells, which might be part of reason for the cytotoxicity too. In general, after three times' oxidization, the ultrasmall GO-3 nanosheets showed the best biocompability and greatest potential for biological applications.

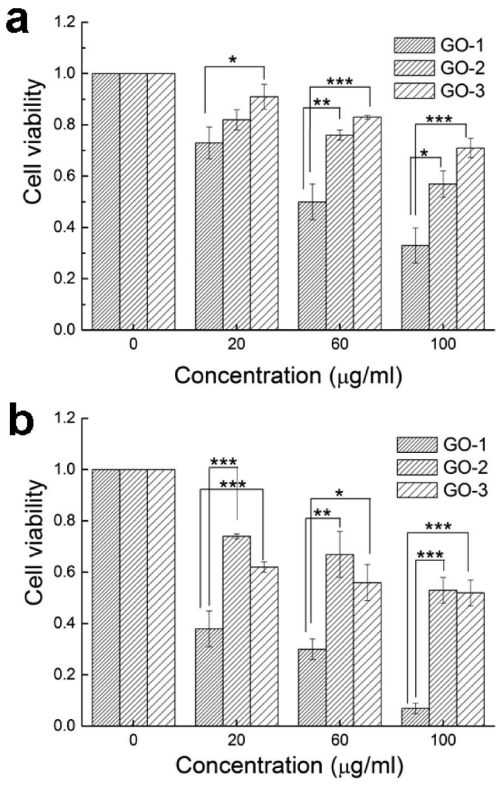

Figure 4. Cell viability of Hela cells treated with three different GO sheets. Incubation with GO nanosheets for 2 h (a) or 24 h (b) at different concentrations, cells were incubated with 1% FBS medium (t-test: ***p < 0.001, **p < 0.01, *p < 0.5).

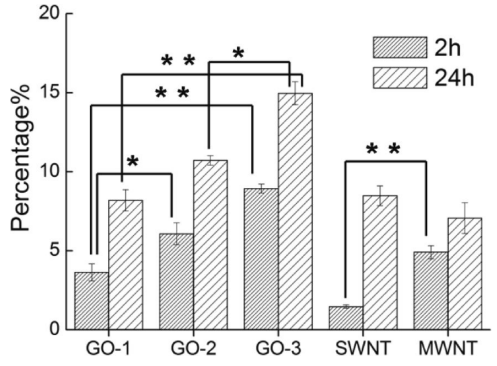

Figure 5. Relative uptake percentages of different materials using isotope labeling method (t-test: ***p < 0.001, **p < 0.01, *p < 0.5).

CONCLUSIONS

We have demonstrated a convenient and high yield method of preparation of uniform ultrasmall GO nanosheets based on a modified Hummers' method. In this study, the $KMnO_4$–H_2SO_4 oxidation was repeatedly used to cut large GO nanosheets into ultrasmall GO nanosheets with lateral size less than 50 nm. Owning to the advantages of the uniform ultrasmall lateral size, the as-prepared GO nanosheets showed intensive fluorescence property and outstanding stability in a wide range of pH values. Significantly, the as-prepared ultrasmall GO nanosheets exhibited lower cytotoxicity and higher cellular uptake amount compared to the random large sized GO nanosheets. These important features suggested that the uniform ultrasmall graphene oxide nanosheets might be a promising nanomaterial

in a range of areas involving cellular imaging, drug delivery, and biosensors.

EXPERIMENTAL SECTION

Preparation of Uniform Sized Ultrasmall GO Nanosheets. The random distributed sized GO nanosheets were prepared from normal graphite powder by a modified Hummers' method. To obtain the uniform ultrasmall GO nanosheets, the as-prepared random distributed sized GO nanosheets should be further oxidized twice. In a typical experiment, graphite powder (4 g) was added to a mixture of concentrated H_2SO_4 (24 mL), $K_2S_2O_8$ (6 g), and P_2O_5 (6 g). After having been stirred for 5 h at 80 °C, the resultant dark blue mixture was slowly cooled to room temperature over a period of about 6 h. The cooled mixture was then diluted to 500 mL with Milli-Q water and filtered through a 0.22 μm membrane, then the filtrate of preoxidized graphite powder was dried overnight at 60 °C. The preoxidized graphite powder (2 g) was added to 150 mL of cold H_2SO_4 (0 °C) and followed by 25 g of $KMnO_4$ being added gradually with stirring in an ice bath. After stirring for 15 min, the mixture was diverted to an oil bath with further stirring for 8 h at 40 °C, and then Milli-Q water (750 mL) and H_2O_2 (30 wt %, 30 mL) were gradually added to terminate the reaction. After standing still overnight the obtained precipitation was washed by diluted hydrochloride acid (1:10 in volume) and Milli-Q water. After centrifugation at 6000 rpm for 10 min, the precipitations were dispersed in Milli-Q water and dialyzed for three days. After being sonicated for 2−3 h at 500 W in an ice bath (lower than 15°C), the obtained brown colloid was normal random distributed sized GO nanosheets, with yield of about 90% (namely GO-1 in the following). For the second oxidization, 2 g of the precipitation (obtained after 6000 rpm centrifugation) of GO-1 was added to 150 mL of cold H_2SO_4 at 0 °C, and 25 g of $KMnO_4$ was added gradually with stirring in an ice bath. After 15 min of stirring, the mixture was diverted to an oil bath with the further stirring 8 h at 40 °C, and then 750 mL of distilled water and 30 mL of H_2O_2 (30 wt %) were added gradually to terminate the reaction. The obtained precipitation (after standing overnight) was washed by diluted hydrochloride acid (1:10 in volume) and Milli-Q water, and the precipitations were dispersed and dialyzed in Milli-Q water for three days and sonicated for 2−3 h at 500 W in an ice bath (<15 °C); the obtained yellow colloid was the middle sized GO-2 nanosheets (yield ~80%). To obtain the ultrasmall GO nanosheets, further oxidization was employed as follows: 2 g of the precipitation (obtained after 8000 rpm centrifugation) of GO-2 was added to 150 mL of cold H_2SO_4 (0 °C), and 25 g of $KMnO_4$ was added gradually with stirring in an ice bath. After stirring for 15 min, the mixture was diverted to an oil bath with further stirring for 8 h at 40 °C, and then distilled water (250 mL) and H_2O_2 (30 wt %, 30 mL) was added gradually to terminate the reaction. After standing still overnight, the obtained precipitation was washed by diluted hydrochloride acid (1:10 in volume) and Milli-Q water. Then the solution was dialyzed for three days and sonicated for 2−3 h at 500 W in an ice bath (<15 °C), and the obtained light yellow colloid was ultrasmall sized GO-3 nanosheets with a yield of ~60%.

Radio-Label Experiments. Three types of GO nanosheets, single-walled carbon nanotubes (SWCNTs), and multi-walled carbon nanotubes (MWCNTs) were labeled with ^{125}I radionuclide by the Chloramine-T (N-chloro-p-toluenesulfonic acid) method. In brief, 1.0 mg/mL of GO-1, GO-2, and GO-3 nanosheets and SWCNTs and 0.5 mg/mL of MWCNTs, respectively, were mixed with $Na^{125}I$, PBS (0.25 M, pH = 7.4) and Chloramine-T (dissolved in 0.25 M PBS) solutions and further sonicated for 30 minutes to ensure successful labeling. The resultant mixtures were dialyzed 24 h to remove the free ^{125}I ions, and the label yield about 60%−70% was determined by paper chromatography (PC, silica gel, eluting solvent: Vacetone:Vwater = 9:1). The radiochemical purities were enhanced up to 96% on average by times of precipitation and resuspension. The radiochemical stability of the labeling nanomaterials indicated that the radiochemical purity was maintained in the range of 85 ± 6% after 2 h incubation in 1% FBS culture medium, which suggested these five nanomaterials were stable enough to study the intracellular uptake. The radioactive intensities of free ^{125}I ions in 1% FBS culture medium were also considered for evaluating the possible influences of ^{125}I detaching.

TEM Characterization. Hela cells were cultured in MEM medium (Invitrogen, Carlsbad, CA, USA) with 10% fetal bovine serum (FBS) and antibiotics (100 μg/mL streptomycin and 100 μg/mL penicillin) at 37 °C under conditions of 5% CO_2. After growing overnight, cells (with a final cell concentration of 10^5/mL) were incubated with 1% FBS/MEM medium, containing 20 or 100 μg/mL GO nanosheets. After 2 h or 24 h, Hela cells were washed three times with PBS, collected, and then fixed with 2.5% glutaraldehyde. The fixed cells were washed with PBS, postfixed with 1% aqueous OsO_4 (Fluka Chemical Corp. of Sigma Aldrich) for 1 h, and washed twice with PBS. Then the cells were dehydrated through an ethanol series (70% for 15 min, 90% for 15 min, and two times with 100% for 15 min) and embedded in Epon/Araldite resin (polymerization at 65 °C for 15 h). Thin sections (~90 nm) containing the cells were placed on the grids, stained for 1 min each with 4% uranyl acetate (1:1 acetone/water in volume) and 0.2% Raynolds lead citrate (in water), air-dried, and then examined by a transmission electron microscope (JEM-1230, JOEL Ltd., Tokyo, Japan).

Isotope Tracing Cellular Uptake Amount. Hela cells were cultured in MEM medium (Invitrogen, Carlsbad, CA, USA) with 10% fetal bovine serum (FBS) and antibiotics (100 μg/mL streptomycin and 100 μg/mL penicillin) at 37 °C under conditions of 5% CO_2. Cells (~5×10^4) were seeded in 24-well plates and grown overnight. The five types of radio-labeled nanomaterials with 1 mL of fresh medium (1% FBS) were added in the well with the final concentration of 20 μg/mL. One group without cells was performed with the same conditions as the control experiment (ctrl 1). Meanwhile, another group of free ^{125}I ions in 1% FBS culture medium in the same conditions was performed as another control experiment (ctrl 2). After incubation for 2 or 24 h at 37 °C, samples in the control group were collected and washed three times with PBS solutions for label intensity measurements, and the other groups with the cell samples were washed three times with PBS solutions to remove the excess radio-labeled nanomaterials. All the washing PBS solutions were collected for radioactive intensity measurements, and all the cells were digested with 0.25% trypsin and resuspended in 1.05 mL of 1% FBS cell medium. Aliquots per 50 μL were taken from the treated samples to determine the number of cells, and the remaining cell suspensions were collected for radioactive intensity measurements to determine the efficiency of cellular uptake. The relative uptake proportion of GO sheets was evaluated by the following equation: $p = R_{sample}/(R_{ctrl\ 1} - R_{ctrl\ 2}) \times 100\%$ (R_{sample}, $R_{ctrl\ 1}$, and $R_{ctrl\ 2}$ represented the activity of reference samples, the activity of control experiment ctrl 1 and ctrl 2, R count per minute; cpm). The up-take quantities of the materials per 10000 cells (ng/10000 cells) were calculated according to the following equation: uptake quantities/10000 cells = $p \times 200000/n$, where p is the percentage of uptake of different materials, n is the number of cells in each sample, and 20000 (ng) is conversion of the primary adding quantity of materials (20 μg/mL).

Cell Culture and Cytotoxicity Test. Hela cells were grown in MEM medium (Invitrogen, Carlsbad, CA, USA) with 10% fetal bovine serum (FBS) and antibiotics (100 μg/mL streptomycin and 100 μg/mL penicillin) at 37 °C under conditions of 5% CO_2. Cells (~5×10^4) were seeded in 24-well plates and grown overnight. Then fresh media (1% FBS) were added with different final concentrations (0, 20, 60, 100 μg/mL) of different GO nanosheets. after incubation for a certain time (2 h or 24 h), 50 μL of 5 mg/mL Thiazolyl Blue tetrazolium bromide (MTT; Sigma-Aldrich, St. Louis, MO, USA) solution was added to each well of the 24-well plate, followed by an additional 4 h incubation at 37 °C. Cells were then lysed with 10% acid sodium dodecyl sulfate (SDS; Sigma) solution. After centrifugation at 14000 rpm for 10 min, 200 μg of the supernatant was taken and measured the absorbance of 570 nm on a microplate reader (model 680; Bio-Rad Hercules, CA, USA).

■ ASSOCIATED CONTENT

Supporting Information

Materials and equipment used in the experiment. More characterizations of the materials and amplified TEM images of cells were included. This material is available free of charge via the Internet at http://pubs.acs.org.

■ AUTHOR INFORMATION

Corresponding Author

*E-mail: huangqing@sinap.ac.cn (Q.H.), nercn.liurui@yahoo.com.cn (R.L.).

Author Contributions

‡These authors contributed equally.

Notes

The authors declare no competing financial interest.

■ ACKNOWLEDGMENTS

This work was financially supported by the National Natural Science Foundation (51102272, U1232113 and 61008056).

■ REFERENCES

(1) Geim, A. K.; Novoselov, K. S. *Nat. Nanotechnol.* **2007**, *6*, 183−191.
(2) Li, D.; Muller, M. B.; Gilje, S.; Kaner, R. B.; Wallace, G. G. *Nat. Nanotechnol.* **2008**, *3*, 101−105.
(3) Lee, C.; Wei, X.; Kysar, J. W.; Hone, J. *Science* **2008**, *321*, 385−388.
(4) Allen, M. J.; Tung, V. C.; Kaner, R. B. *Chem. Rev.* **2010**, *110*, 132−145.
(5) Eda, G.; Fanchini, G.; Chhowalla, M. *Nat. Nanotechnol.* **2008**, *3*, 270−274.
(6) Li, X. L.; Wang, X. R.; Zhang, L.; Lee, S. W.; Dai, H. J. *Science* **2008**, *319*, 1229−1232.
(7) Stankovich, S.; Dikin, D. A.; Dommett, G. H. B.; Kohlhaas, K. M.; Zimney, E. J.; Stach, E. A.; Piner, R. D.; Nguyen, S. T.; Ruoff, R. S. *Nature* **2006**, *442*, 282−286.
(8) Compton, O. C.; Nguyen, S. T. *Small* **2010**, *6*, 711−723.
(9) Li, D.; Kaner, R. B. *Science* **2008**, *320*, 1170−1171.
(10) Kim, H.; Abdala, A. A.; Macosko, C. W. *Macromolecules* **2010**, *43*, 6515−6530.
(11) Lu, C. H.; Yang, H. H.; Zhu, C. L.; Chen, X.; Chen, G. N. *Angew. Chem., Int. Ed.* **2009**, *48*, 4785−4787.
(12) He, S.; Song, B.; Li, D.; Zhu, C.; Qi, W.; Wen, Y.; Wang, L.; Song, S.; Fang, H.; Fan, C. *Adv. Funct. Mater.* **2010**, *20*, 453−459.
(13) Wang, H.; Zhang, Q.; Chu, X.; Chen, T.; Ge, J.; Yu, R. *Angew. Chem., Int. Ed.* **2011**, *50*, 7065−7069.
(14) Singh, G.; Choudhary, A.; Haranath, D.; Joshi, A. G.; Singh, N.; Singh, S.; Pasricha, R. *Carbon* **2012**, *50*, 385−394.
(15) Zhang, M.; Yin, B. C.; Tan, W. H.; Ye, B. C. *Biosens. Bioelectron.* **2011**, *26*, 3260−3265.
(16) Feng, L. Z.; Zhang, S. A.; Liu, Z. A. *Nanoscale* **2011**, *3*, 1252−1257.
(17) Feng, L.; Liu, Z. *Nanomedicine* **2011**, *6*, 317−324.
(18) Wang, X.; Zhi, L.; Mullen, K. *Nano Lett.* **2007**, *8*, 323−327.
(19) Latorre-Sanchez, M.; Atienzar, P.; Abellan, G.; Puche, M.; Fornes, V.; Ribera, A.; Garcia, H. *Carbon* **2012**, *50*, 518−525.
(20) Chen, H.; Muller, M. B.; Gilmore, K. J.; Wallace, G. G.; Li, D. *Adv. Mater.* **2008**, *20*, 3557−3561.
(21) Soldano, C.; Mahmood, A.; Dujardin, E. *Carbon* **2010**, *48*, 2127−2150.
(22) Dreyer, D. R.; Park, S.; Bielawski, C. W.; Ruoff, R. S. *Chem. Soc. Rev.* **2010**, *39*, 228−240.
(23) Dikin, D. A.; Stankovich, S.; Zimney, E. J.; Piner, R. D.; Dommett, G. H. B.; Evmenenko, G.; Nguyen, S. T.; Ruoff, R. S. *Nature* **2007**, *448*, 457−460.
(24) Zhang, L. M.; Xia, J. G.; Zhao, Q. H.; Liu, L. W.; Zhang, Z. J. *Small* **2010**, *6*, 537−544.
(25) Kotchey, G. P.; Allen, B. L.; Vedala, H.; Yanamala, N.; Kapralov, A. A.; Tyurina, Y. Y.; Klein-Seetharaman, J.; Kagan, V. E.; Star, A. *ACS Nano* **2011**, *5*, 2098−2108.
(26) Song, Y. J.; Qu, K. G.; Zhao, C.; Ren, J. S.; Qu, X. G. *Adv. Mater.* **2010**, *22*, 2206−2210.
(27) Liu, K. P.; Zhang, J. J.; Cheng, F. F.; Zheng, T. T.; Wang, C. M.; Zhu, J. J. *J. Mater. Chem.* **2011**, *21*, 12034−12040.
(28) Yang, X. Y.; Wang, Y. S.; Huang, X.; Ma, Y. F.; Huang, Y.; Yang, R. C.; Duan, H. Q.; Chen, Y. S. *J. Mater. Chem.* **2011**, *21*, 3448−3454.
(29) Duch, M. C.; Budinger, G. R. S.; Liang, Y. T.; Soberanes, S.; Urich, D.; Chiarella, S. E.; Campochiaro, L. A.; Gonzalez, A.; Chandel, N. S.; Hersam, M. C.; Mutlu, G. M. *Nano Lett.* **2011**, *11*, 5201−5207.
(30) Rana, V. K.; Choi, M. C.; Kong, J. Y.; Kim, G. Y.; Kim, M. J.; Kim, S. H.; Mishra, S.; Singh, R. P.; Ha, C. S. *Macromol. Mater. Eng.* **2011**, *296*, 131−140.
(31) Liu, Y.; Yu, D. S.; Zeng, C.; Miao, Z. C.; Dai, L. M. *Langmuir* **2010**, *26*, 6158−6160.
(32) Singh, S. K.; Singh, M. K.; Kulkarni, P. P.; Sonkar, V. K.; Grácio, J. J. A.; Dash, D. *ACS Nano* **2012**, *6*, 2731−2740.
(33) Sun, X. M.; Liu, Z.; Welsher, K.; Robinson, J. T.; Goodwin, A.; Zaric, S.; Dai, H. J. *Nano Res.* **2008**, *1*, 203−212.
(34) Liu, Z.; Robinson, J. T.; Sun, X. M.; Dai, H. J. *J. Am. Chem. Soc.* **2008**, *130*, 10876−10877.
(35) Lu, C.-H.; Zhu, C.-L.; Li, J.; Liu, J.-J.; Chen, X.; Yang, H.-H. *Chem. Commun.* **2010**, *46*, 3116−3118.
(36) Yang, K.; Zhang, S.; Zhang, G.; Sun, X.; Lee, S.-T.; Liu, Z. *Nano Lett.* **2010**, *10*, 3318−3323.
(37) Peng, C.; Hu, W.; Zhou, Y.; Fan, C.; Huang, Q. *Small* **2010**, *6*, 1686−1692.
(38) Hong, H.; Yang, K.; Zhang, Y.; Engle, J. W.; Feng, L.; Yang, Y.; Nayak, T. R.; Goel, S.; Bean, J.; Theuer, C. P.; Barnhart, T. E.; Liu, Z.; Cai, W. *ACS Nano* **2012**, *6*, 2361−2370.
(39) Wang, Y.; Lu, J.; Tang, L. H.; Chang, H. X.; Li, J. H. *Anal. Chem.* **2009**, *81*, 9710−9715.
(40) Wang, L.; Pu, K.-Y.; Li, J.; Qi, X.; Li, H.; Zhang, H.; Fan, C.; Liu, B. *Angew. Chem., Int. Ed.* **2011**, *23*, 4386−4391.
(41) Robinson, J. T.; Tabakman, S. M.; Liang, Y.; Wang, H.; Sanchez Casalongue, H.; Vinh, D.; Dai, H. *J. Am. Chem. Soc.* **2011**, *133*, 6825−6831.
(42) Tian, B.; Wang, C.; Zhang, S.; Feng, L.; Liu, Z. *ACS Nano* **2011**, *5*, 7000−7009.
(43) Sun, X.; Luo, D.; Liu, J.; Evans, D. G. *ACS Nano* **2010**, *4*, 3381−3389.
(44) Wang, X.; Bai, H.; Shi, G. *J. Am. Chem. Soc.* **2011**, *133*, 6338−6342.
(45) Luo, J. Y.; Cote, L. J.; Tung, V. C.; Tan, A. T. L.; Goins, P. E.; Wu, J. S.; Huang, J. X. *J. Am. Chem. Soc.* **2010**, *132*, 17667−17669.
(46) Hu, W.; Peng, C.; Lv, M.; Li, X.; Zhang, Y.; Chen, N.; Fan, C.; Huang, Q. *ACS Nano* **2011**, *5*, 3693−3700.
(47) Kosynkin, D. V.; Higginbotham, A. L.; Sinitskii, A.; Lomeda, J. R.; Dimiev, A.; Price, B. K.; Tour, J. M. *Nature* **2009**, *458*, 872−876.
(48) Hummers, W. S.; Offeman, R. E. *J. Am. Chem. Soc.* **1958**, *80*, 1339−1339.
(49) Marcano, D. C.; Kosynkin, D. V.; Berlin, J. M.; Sinitskii, A.; Sun, Z. Z.; Slesarev, A.; Alemany, L. B.; Lu, W.; Tour, J. M. *ACS Nano* **2010**, *4*, 4806−4814.
(50) Kudin, K. N.; Ozbas, B.; Schniepp, H. C.; Prud'homme, R. K.; Aksay, I. A.; Car, R. *Nano Lett.* **2008**, *8*, 36−41.
(51) Chien, C.-T.; Li, S.-S.; Lai, W.-J.; Yeh, Y.-C.; Chen, H.-A.; Chen, I. S.; Chen, L.-C.; Chen, K.-H.; Nemoto, T.; Isoda, S.; Chen, M.; Fujita, T.; Eda, G.; Yamaguchi, H.; Chhowalla, M.; Chen, C.-W. *Angew. Chem., Int. Ed.* **2012**, *51*, 1−6.
(52) Bosi, S.; Da Ros, T.; Spalluto, G.; Prato, M. *Eur. J. Med. Chem.* **2003**, *38*, 913−923.
(53) Nakamura, E.; Isobe, H. *Acc. Chem. Res.* **2003**, *36*, 807−815.
(54) Li, J.; Zhu, Y.; Li, W.; Zhang, X.; Peng, Y.; Huang, Q. *Biomaterials* **2010**, *31*, 8410−8418.

(55) Liu, Z.; Tabakman, S.; Welsher, K.; Dai, H. *Nano Res.* **2009**, *2*, 85−120.
(56) Mu, Q.; Su, G.; Li, L.; Gilbertson, B.; Yu, L. H.; Zhang, Q.; Sun, Y.; Yan, B. *ACS Appl. Mater. Interfaces* **2012**, *4*, 2259−2266.
(57) Zhu, Y.; Li, W.; Li, Q.; Li, Y.; Li, Y.; Zhang, X.; Huang, Q. *Carbon* **2009**, *47*, 1351−1358.
(58) Hu, W.; Peng, C.; Luo, W.; Lv, M.; Li, X.; Li, D.; Huang, Q.; Fan, C. *ACS Nano* **2010**, *4*, 4317−4323.
(59) Akhavan, O.; Ghaderi, E. *ACS Nano* **2010**, *4*, 5731−5736.